Numerical Optimization of Internal Geometry for Additively Manufactured Hydraulic Manifolds

Jan Bartolj,[1] Katharina Schmitz,[2]
Nikola Vukašinović,[1] Franc Majdič[1]

[1] University of Ljubljana, Faculty of Mechanical Engineering, Ljubljana, Slovenia
jan.bartolj@fs.uni-lj.si, nikola.vukasinovic@fs.uni-lj.si, franc.majdic@fs.uni-lj.si
[2] RWTH Aachen University, Institute for Fluid Power Drives and Systems, Aachen, Germany
Katharina.Schmitz@ifas.rwth-aachen.de

This study presents a novel approach for the design and optimisation of hydraulic manifolds with self-supporting geometries that are compatible with additive manufacturing. Conventional manifolds with a circular cross-section often require complex post-processing as the internal channels are not supported. In this work, configurations of cross-sectional shapes that do not require support structures are investigated. A parametric optimisation and an adjoint gradient algorithm strategy were implemented to refine the cross-sectional geometry of the internal channels with the aim of minimising pressure loss while ensuring manufacturability. Use of CFD simulations to analyse the flow behaviour and pressure losses for different design variants. The integration of self-supporting features not only improves flow efficiency but also realises the full potential of AM by reducing manufacturing time and post-processing requirements. This research contributes to the development of more efficient, production-ready hydraulic systems through simulation-based design methods that take cross-sectional geometry into account.

DOI
https://doi.org/10.18690/um.fs.7.2025.4

ISBN
978-961-299-049-7

Keywords:
hydraulic manifold, additive manufacturing, internal cross-section, parametrical optimization, CFD simulation

University of Maribor Press

1 Introduction

The European Union's legislative framework, particularly the Energy Efficiency Directive (EU 2023/1791) and the Ecodesign Directive (2009/125/EC), sets increasingly strict targets for reducing energy consumption in industry. These policies not only drive improvements in components like pumps and hydraulic systems but also push for new design methods that prioritize energy performance across a product's lifecycle.

In hydraulic systems, internal flow losses in manifolds represent a non-negligible source of inefficiency. Traditional design methods are largely constrained by manufacturing limits, resulting in geometries that are rarely optimal from a fluid dynamics standpoint. With the rise of Additive Manufacturing (AM), and particularly metal-based techniques such as SLM (Selective Laser Melting) or DMLS (Direct Metal Laser Sintering), designers are no longer limited to planar drilling or simple intersections [3]. Instead, AM allows for the fabrication of fully three-dimensional internal channels, opening up the design space for true geometry-driven optimization [1], [2], [4].

The work presented here combines numerical methods for shape optimisation, in particular parametric optimisation and adjoint gradient techniques, with the design freedom offered by AM. Whilst AM allows for complex geometries[5, 6], it also brings its own limitations, such as the need for support structures during manufacture. For applications with internal flow, such as manifolds, it can be difficult or impossible to remove these supports and must therefore be considered early in the design process. Despite these challenges, AM remains an important enabler, allowing flow paths to be designed according to performance rather than manufacturing constraints.

2 Background & Motivation

2.1 Energy consumption in hydraulics

In hydraulics energy consumption is usually defined by the input energy needed to generate and maintain flow of the fluid under pressure. So basically, energy consumption is a sum of all losses in the hydraulic circuit. Mainly, losses occur where

mechanical or electrical power is used to drive hydraulic pumps, losses caused by friction, turbulence and changes in fluid flow direction, pressure drops and heat generation.

2.2 Numerical simulations

The flow simulations were based on the incompressible, stationary Navier–Stokes equations, which were solved using the finite volume method. The fluid was assumed to be a Newtonian fluid with constant properties. Turbulence was modelled using the realisable k-ω SST model, which is suitable for internal flows with moderate curvature and separation. The governing equations include conservation of mass (1):

$$\nabla \cdot \mathbf{u} = 0 \tag{1}$$

and momentum conservation (2):

$$\rho(\mathbf{u} \cdot \nabla)\mathbf{u} = -\nabla p + \nabla \cdot \bar{\boldsymbol{\tau}} + \mathbf{F} \tag{2}$$

where $\mathbf{u}$ is the velocity vector, p the pressure, ρ the density, $\bar{\boldsymbol{\tau}}$ Newtonian viscous stress tensor and $\mathbf{F}$ represents additional body forces.

Pressure-velocity coupling was handled using the SIMPLE algorithm. Boundary conditions were defined as velocity inlets and pressure outlets, with no-slip conditions on all walls. Meshes were unstructured with refined boundary layers; y+ values were monitored to maintain compatibility with wall functions. Simulation outputs primarily pressure drop served as the objective function for optimization in both parametric and adjoint-based workflows.

2.3 Gradient Adjoint method

The Gradient Adjoint method (GA-method) efficiently calculates how an objective function changes in relation to shape variations (Figure 1).

Unlike finite differences, which require many flow simulations, the GA-method solves a single additional system, regardless of the number of design variables. This makes it ideal for optimising complex geometries with many parameters. The

method provides accurate gradients at low cost, enabling effective workflows for shape optimisation.

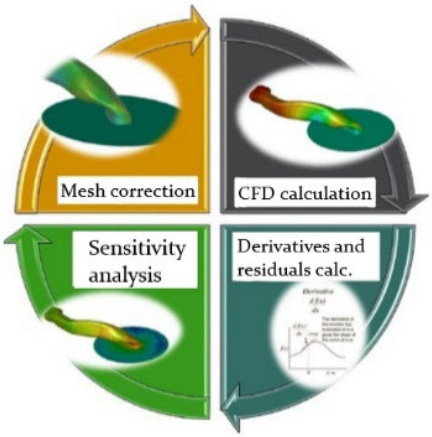

Figure 1: Gradient Adjoint method workflow.

The GA-method in ANSYS Fluent computes sensitivities of an objective function J with respect to shape changes by solving the adjoint form of the flow equations. Starting from the primal residual (3):

$$\mathbf{R}(\mathbf{U}) = 0\,. \tag{3}$$

where $\mathbf{U}$ is the flow solution vector, the adjoint variables $\boldsymbol{\lambda}$ are found by solving equation (4):

$$\left(\frac{\partial \mathbf{R}}{\partial \mathbf{U}}\right)^{\mathrm{T}} \boldsymbol{\lambda} = \frac{\partial J}{\partial \mathbf{U}}\,. \tag{4}$$

The shape derivative, which represents the gradient of the objective function with respect to boundary displacement $\delta\mathbf{x}$, is then obtained from equation (5):

$$\frac{dJ}{d\mathbf{x}} = \frac{\partial J}{\partial \mathbf{x}} - \boldsymbol{\lambda}^{\mathrm{T}} \frac{\partial \mathbf{R}}{\partial \mathbf{x}}\,. \tag{5}$$

This expression allows efficient calculation of gradients for complex geometries without repeating full flow simulations for each parameter. The computed gradients are used to drive mesh deformation and guide shape optimization, relying on steady-state RANS flow solutions and consistent turbulence modelling.

3 Methodology

Research is divided into two case studies. Both are based on the geometry you can see in the Figure 2.

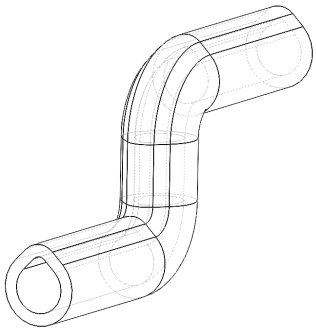

Figure 2: Base S-bend channel geometry for optimisation.

It is a simple S-shaped channel, as often found in hydraulic manifolds. We wanted this geometry to be simple, so we chose to have both bends in the same reference plane. Overall simulations of this S-bent shape are L = 115 mm, H = 70 mm, W = 20 mm.

The first case study is fully parametric and tied to the basic dimension of the geometry, while the second case study is based on the fluid-filled cavity within the channel itself.

3.1 Parametric optimization case 1

A basic teardrop shape with a cross-section of 120 mm^2 was used and 3 measurements were used for parameter optimization. The measurements selected are shown in Figure 3. The top measurement is the upper radius. This is defined as

2 mm, while the second measurement is defined as the angle of the conical upper part of the teardrop and is 90°. The last measurement is again the radius, but this time the lower circular part is defined and is shown in Figure 3 as 6 mm.

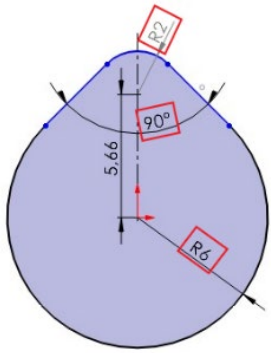

Figure 3: Case study 1. Parametrical optimization of the teardrop shape.

3.2 Gradient adjoint simulation case

The optimisation process using the GA-method is slightly different from the parametric simulation in the previous case. This time we need to define the actual fluid domain as this process optimises the entire fluid geometry within a channel and is not limited to different dimensionally defined sketches. We have the geometry in Figure 4.

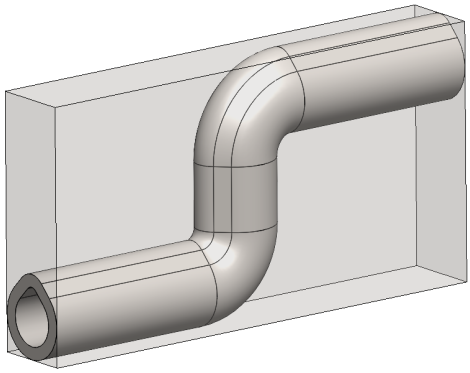

Figure 4: Case study 2. GA-method base geometry with defined optimization space.

4 Implementation

4.1 Mesh

The mesh we used was unstructured with polyhedral elements across the entire geometry. We used boundary layers near the walls of the fluid region as a refinement to better understand the conditions that occur near the fluid-wall interface. This study confirmed that a cell number of about 550 thousand was sufficient in our case to efficiently describe the flow conditions without wasting computation time.

4.2 Solvers and governing equations

The Ansys Fluent solver was used in all cases to calculate the CFD results. This is a CFD solver based on the finite volume method. The numerical formulation used was calculated for incompressible, steady state, Newtonian, isothermal, single-phase, turbulent flow. This meant that two Navier-Stokes equations for mass and momentum conservation were used in combination with the k-ω SST turbulence model.

4.3 Boundary conditions

In the calculations, we have used water as the hydraulic fluid, with a density of 998 kg/m^3 at room temperature. The fluid we have defined has a kinematic viscosity of $0.993 * 10^{-6}$ m^2/s. Since we did not calculate thermodynamic effects such as heat transfer between the fluid and solid walls, the material of the pipe was not defined.

Calculation domain can be divided into three parts. Main calculation domain of the defined S-bend with two appendices, one per inlet and outlet (see Figure 5). The attachments were added to ensure that the flow at the inlet is fully developed in the actual geometry and the results are not influenced by the boundary surface at the outlet.

At the inlet (yellow in Figure 5) we have defined an inlet velocity of the hydraulic fluid corresponding to the flow rate of 70 l/min. An atmospheric pressure of 101.3 MPa was defined at the outlet (red area in Figure 5). At the interfaces of the fluid area and the attachments at the inlet and outlet (blue and green areas in Figure 5),

we inserted measurement points to effectively calculate the pressure losses and other parameters at the actual inlet and outlet of the observed area.

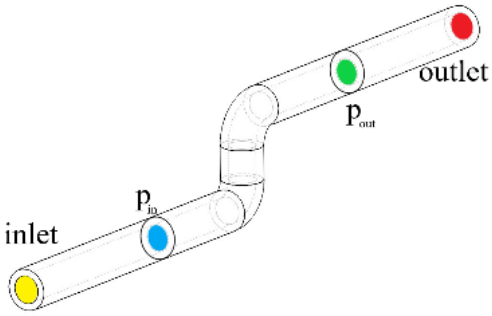

Figure 5: Definition of base geometry appendices with inlet, outlet and measuring areas defined.

5 Results

5.1 Case study 1

It was expected that the result of the first case study would be an enlargement of the fluid area and the elimination of the upper conical edges that define the teardrop shape. As can be seen in Figure 6, this was the case. The optimisation software attempted to make the base circle of the teardrop slightly larger and the upper edges lower. This larger cross-sectional area reduces the velocity through the channel while simultaneously reducing the pressure drop. The resulting change in geometry can be seen in Figure 6 where grey area represents the non-optimized shape, while blue outline, enhanced with the green and red arrows, represents recommended geometry change.

Looking at the flow velocity profiles, it can be seen that this case study slightly improves the channel properties. This becomes clear after the first bend, where a reduced recirculation area can be observed. Less recirculation means less turbulence and a lower pressure drop as the fluid flow is better controlled. The upper velocity profile in Figure 7, profile a) represents the original, non-optimised shape of the teardrop channel, while the lower profile b) represents the optimised shape of the

teardrop channel with an increased angle of the conical part and an upper radius of approx. 4 mm, which is almost twice as large as the initial value.

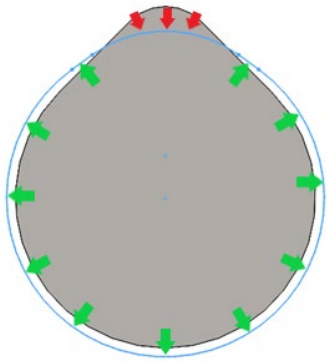

Figure 6: Case study 1 resulting geometry.

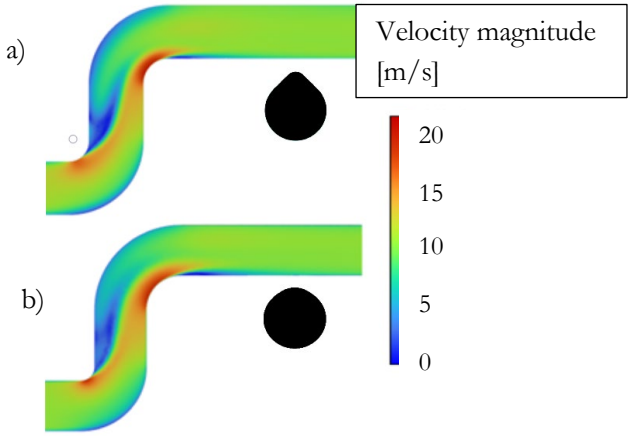

Figure 7: CS1 – Velocity longitudinal profiles comparison with a) non-optimized and b) optimized geometries.

Looking at the parameter of turbulent kinetic energy dissipation, we can compare a) the original and b) the optimised shape of the channel in Figure 8. We can observe the difference in flow behaviour, which confirms the statement obtained from the velocity profiles that the amount of fluid that is recirculating after the first bend decreases.

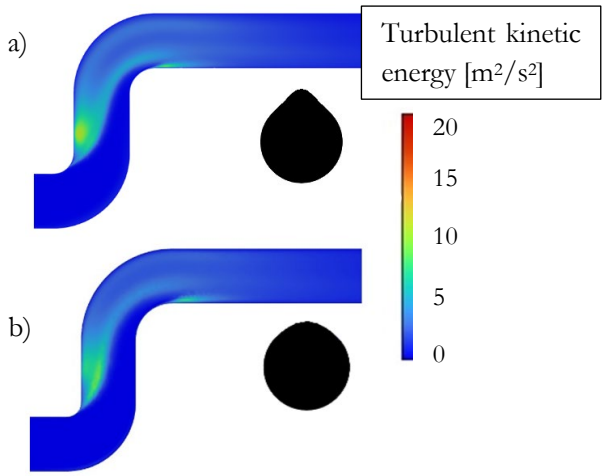

Figure 8: CS1 – Turbulent kinetic energy dissipation longitudinal profiles comparison with a) non-optimized and b) optimized geometries.

If we look at the result of the optimisation itself, we can observe how the different parameters chosen for the optimisation affect the resulting pressure drop on the Figure 9. The first graph represents the response surface that was calculated using the angle of the conical tip of the teardrop and the upper radius and its effect on the resulting pressure drop. It is interesting to note that we can see the local minimum of the response surface. This means that there is a local minimum in the observed set of parameters. At 70 l/min, the original teardrop had a pressure drop of 39412.52 Pa, while the optimised variant has a pressure drop of 33839.58 Pa. By optimising the cross-sectional shape of the geometry alone, a 15 % reduction in pressure loss can be achieved. It is interesting to note that the duct with a circular shape and a cross-sectional area of 120 mm² has a pressure loss of 34697.08 Pa and therefore performs slightly worse than the optimised shape. However, this is not a fair comparison, as the optimisation has increased the cross-sectional area by around 11 %, as already mentioned.

Comparing the response surface diagram for the conical upper angle and the lower radius in Figure 10, we can see that a local minimum is reached again. What is interesting in this case is that the gradients located around the local minimum are much higher than those observed in the previous graph, which makes the local minimum even clearer.

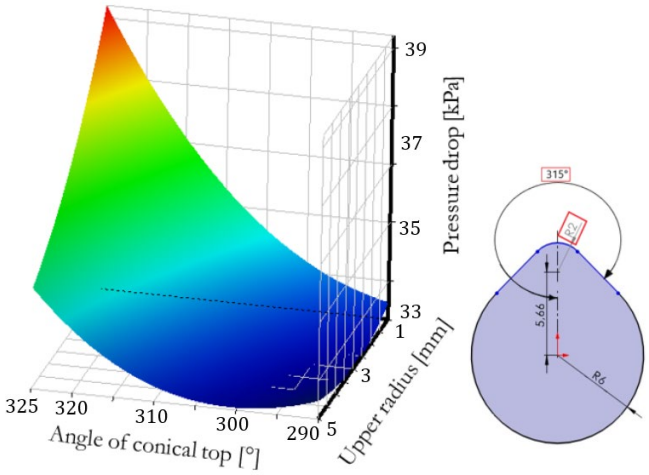

Figure 9: CS1 – Response surface of the parametric study combining angled conical top and upper radius and their effect on pressure drop.

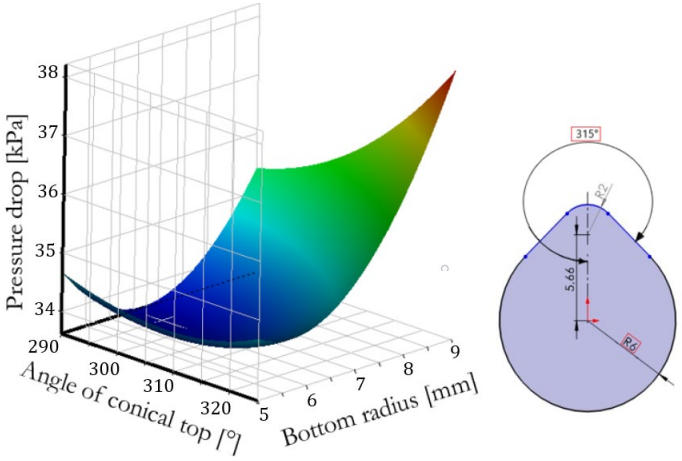

Figure 10: CS1 – Response surface of the parametric study combining angled conical top and bottom radius and their effect on pressure drop.

At the end of case study 1, we have effectively reduced the pressure drop from 39.41 kPa to 33.83 kPa and Turbulent kinetic energy dissipation. With these values, we have reached the local minimum in the response surface and thus the point that gives us the optimal shape of the geometry.

5.3 Case study 2

In this case the optimisation was not purely parametric, but changed the mesh while the CFD results were calculated. Interestingly, the shape obtained with the GA-method has an extremely optimised and almost organic shape. The resulting geometry is shown in green colour in Figure 11, while the transparent grey colour represents the non-optimised geometry.

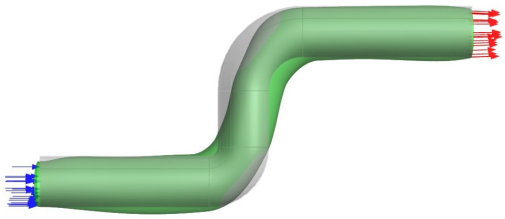

Figure 11: CS2 – Recommended geometry changes as the result of the GA study.

If we look at the velocity profiles of the optimised b) and the non-optimised a) velocity profiles in Figure 12, we can clearly see that the geometry optimisation has effectively reduced the velocity.

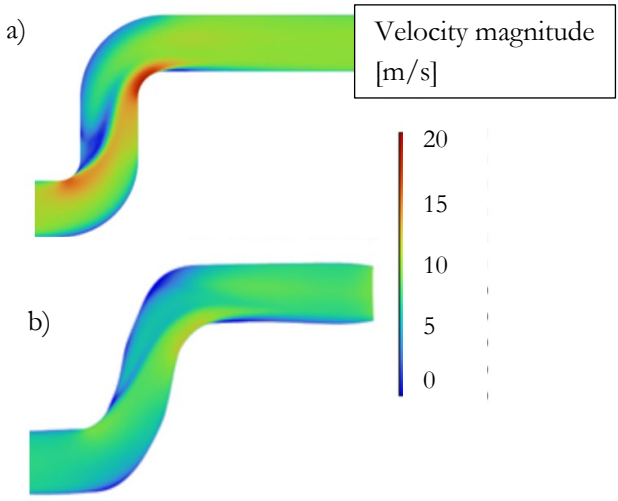

Figure 12: CS2 - Velocity longitudinal profiles comparison with a) non-optimized and b) optimized geometries.

This is mainly due to the increase in the overall circumference of the pipe and the bending of the vertical section to control the flow impact.

Turbulent kinetic energy dissipation that was obtained through this study has shown drastically lower values compared to original geometry. This is why we decided to show the results by themselves in the Figure 13. Maximum calculated value is 3 m^2/s^2. Small amount of recirculation can be spotted at such a smaller scale and the highest value is clearly depicted in red after the second bend where we were expecting some flow separation.

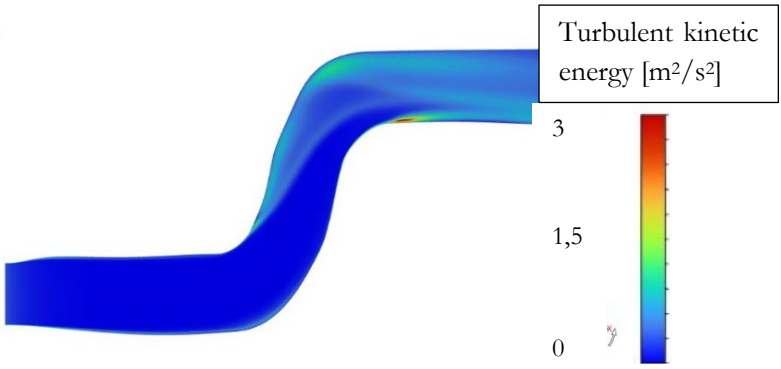

Figure 13: CS2 – Turbulent kinetic energy dissipation longitudinal profile of GA optimized geometry.

In case study 2, the pressure drop was reduced from 39.41 kPa to 30.32 kPa. If this study were to be run further, the result could be even better, but at the expense of extremely morphed mesh elements. It is also very interesting that in this study it was possible for different parts to have different shapes across the entire geometry. This can be seen at the beginning, where the channel must be self-supporting to fulfil the printability criteria, but not self-supporting in the vertical section, where this is not mandatory.

6 Discussion

In this article, we present two case studies in which we effectively improved the flow properties of the simple S-bend channel geometry. One study was parametric and one was performed using the gradient adjoint method. In both studies, we reduced

the pressure drop by about 25 % by changing the geometry of the pipe. In the second case study, we demonstrated the use of the Gradient Adjoint method, which reshapes the elements of the mesh after each design iteration to achieve a more efficient result by determining the critical parts of the geometry. This leads to an optimised shape of the geometry, but also to some shapes that are difficult to produce without the use of additive manufacturing.

All in all, this article shows the great potential that numerical optimisation has in industry. Sometimes optimisation should only be used to get an idea for further development, but in some cases these optimised designs could be used directly in a new and improved generation of fluid power components.

References

[1] Arena, M., Ambrogiani, P., Raiola, V., Bocchetto, F., Tirelli, T., & Castaldo, M. (2023). Design and qualification of an additively manufactured manifold for aircraft landing gears applications. *Aerospace, 10*(69), 1–18. https://doi.org/10.3390/aerospace10010069

[2] Biedermann, M. (2022). *Automated design of additive manufactured flow components* (Doctoral thesis, ETH Zurich). https://doi.org/10.3929/ethz-b-000587405

[3] Diegel, O., Nordin, A., & Motte, D. (2019). *A practical guide to design for additive manufacturing.* Springer Singapore. https://doi.org/10.1007/978-981-13-8282-6

[4] Hofmann, U., Fankhauser, M., Willen, S., Inniger, D., Klahn, C., Löffel, K., & Meboldt, M. (2023). Design of an additively manufactured hydraulic directional spool valve: An industrial case study. *Virtual and Physical Prototyping, 18*(1), 1–18. https://doi.org/10.1080/17452759.2023.2166634

[5] Matthiesen, G., Merget, D., Rückert, M., Schmitz, K., & Schleifenbaum, J. H. (2018). Additive manufacturing processes in fluid power – properties and opportunities demonstrated at a flow-optimized fitting. In *Proceedings of the International Conference on Hydraulics and Pneumatics – HERVEX* (pp. 1–6). ISSN 1454-8003

[6] Tappeiner, Z., Donners, M., Schmid, M., & Schmitz, K. (2014, October). Resource saving process route for integrated hydraulic components. *HyRess Project poster*, RWTH Aachen University. Retrieved July 30, 2025, from https://acam.rwth-campus.com/wp-content/uploads/sites/11/2014/10/HyRess-Resource-saving-Process-Route-for-Integrated-Hydraulic-Components.pdf